Title

Arabidopsis Root-Type Ferredoxin:NADP(H) Oxidoreductase 2 Is Involved in Detoxification of Nitrite in Roots

Running head

Detoxification of nitrite by root FNR2

Corresponding author

Takushi Hachiya

RIKEN Center for Sustainable Resource Science, 1-7-22 Suehiro-cho, Tsurumi-ku, Yokohama, Kanagawa 230-0045, Japan

Fax: +81-45-503-9609

e-mail: hachiya.takushi@h.mbox.nagoya-u.ac.jp

Subject areas

(2) Environmental and stress responses

Number of

Black and white figures: 2

Color figures: 3

Tables: 0

Number of supplementary materials: 5

Title

Arabidopsis Root-Type Ferredoxin:NADP(H) Oxidoreductase 2 Is Involved in Detoxification of Nitrite in Roots

Running head

Detoxification of nitrite by root FNR2

Author

Takushi Hachiya[1,2], Nanae Ueda[1], Munenori Kitagawa[3], Guy Hanke[4], Akira Suzuki[5], Toshiharu Hase[6] and Hitoshi Sakakibara[1,2]

Author's addresses

[1]RIKEN Center for Sustainable Resource Science, 1-7-22 Suehiro-cho, Tsurumi-ku, Yokohama, Kanagawa 230-0045, Japan, [2]Department of Biological Mechanisms and Functions, Graduate School of Bioagricultural Sciences, Nagoya University, Nagoya, Aichi 464-8601, Japan, [3]Cold Spring Harbor Laboratory, Cold Spring Harbor, New York 11724, [4]School of Biological and Chemical Sciences, Queen Mary University of London, Mile End Road, 7 London E1 4NS, UK, [5]INRA, Institut Jean-Pierre Bourgin, UMR1318, ERL CNRS 3559, Saclay Plant Sciences, RD10, F-78026 Versailles, France, [6]Laboratory of Regulation of Biological Reaction, Institute for Protein Research, Osaka University, Suita, Osaka, 565-0871 Japan

Abbreviations

FNR, ferredoxin:NADP(H) oxidoreductse; Fd, ferredoxin; G6PD, glucose-6-phosphate dehydrogenase; GOGAT, glutamine-oxoglutarate aminotransferase; GS, glutamine synthetase; GUS, β-glucuronidase; N, nitrogen; NiR, nitrite reductase; NO, nitric oxide;

NR, nitrate reductase; NRT, nitrate transporter; oxPPP, oxidative pentose phosphate pathway; Q-PCR, quantitative reverse transcription polymerase chain reaction; RT-PCR, reverse transcription polymerase chain reaction

Footnotes

The nucleotide sequence reported in this paper has been submitted to The Arabidopsis Information Resource (TAIR) under accession numbers

Abstract

Ferredoxin : NADP(H) oxidoreductase (FNR) plays a key role in redox metabolism in plastids. Whereas leaf FNR (LFNR) is required for photosynthesis, root FNR (RFNR) is believed to provide electrons to ferredoxin (Fd)-dependent enzymes, including nitrite reductase (NiR) and Fd-glutamine-oxoglutarate aminotransferase (Fd-GOGAT) in non-photosynthetic conditions. In some herbal species, however, most nitrate reductase activity is located in photosynthetic organs, and ammonium in roots is assimilated mainly by Fd-independent NADH-GOGAT. Therefore, RFNR might have a limited impact on N assimilation in roots grown with nitrate or ammonium nitrogen sources. *AtRFNRs* are rapidly induced by application of toxic nitrite. Thus, we tested the hypothesis that RFNR could contribute to nitrite reduction in roots by comparing *A. thaliana* seedlings of wild type with loss-of-function mutants of *RFNR2*. When these seedlings were grown under nitrate, nitrite or ammonium, only nitrite nutrition caused impaired growth and nitrite accumulation in roots of *rfnr2*. Supplementation of nitrite with nitrate or ammonium as N sources did not restore the root growth in *rfnr2*. Also, a scavenger for nitric oxide (NO) could not effectively rescue the growth impairment. Thus, nitrite toxicity, rather than N depletion or nitrite-dependent NO production, probably causes the *rfnr2* root growth defect. Our results strongly suggest that RFNR2 has a major role in reduction of toxic nitrite in roots. A specific set of genes related to nitrite reduction and the supply of reducing power responded to nitrite concomitantly, suggesting that the products of these genes act cooperatively with RFNR2 to reduce nitrite in roots. (249 words)

Keywords: ferredoxin:NADP(H) oxidoreductse, ferredoxin, nitrite reduction, root-type

isoform

Introduction

111 Ferredoxin : NADP(H) oxidoreductase (FNR) plays a key role in redox
112 metabolism in plastids (Hanke and Mulo 2013). In chloroplasts, FNR oxidizes the
113 reduced form of ferredoxin (Fd) to reduce $NADP^+$, which in turn, supplies the Calvin
114 cycle with NADPH. In non-photosynthetic plastids, FNR reduces Fd using NADPH
115 derived from the oxidative pentose phosphate pathway (oxPPP), providing reducing
116 power for various biosynthetic processes such as assimilatory pathways of nitrogen (N),
117 sulfur and fatty acids. These opposing reactions are believed to be catalyzed by specific
118 FNR isoproteins, i.e. leaf FNR (LFNR) and root FNR (RFNR), respectively (Hanke et al.
119 2004, Hanke et al. 2005). In *Arabidopsis thaliana*, loss-of-function of *AtLFNRs* impaired
120 autotrophic growth and photosynthetic capacity, demonstrating their essential roles in
121 operating the electron flow *in vivo* (Lintala et al. 2009, Lintala et al. 2012). By contrast,
122 the physiological importance of RFNR remains to be investigated using knock-out
123 mutants.

124 N assimilation requires a large amount of reducing power. The Fd-dependent
125 enzymes in this pathway include nitrite reductase (NiR) and Fd-glutamine-oxoglutarate
126 aminotransferase (Fd-GOGAT). Given that expression of *AtRFNRs* (*RFNR1*; At4g05390,
127 *RFNR2*; At1g30510, see Hanke et al. 2005) are induced by application of either nitrate or
128 ammonium (Wang et al. 2000, 2003, Patterson et al. 2010), AtRFNRs could provide
129 reducing equivalents to N assimilation in roots. In some herbal species, however, nitrate
130 is reduced predominantly in shoots using the reducing equivalents derived from
131 photosynthesis (Scheurwater et al. 2002, Bloom et al. 2010). Nitrate reductase (NR)
132 activities of hydroponically grown *A. thaliana* were much higher in shoots than roots

(Rachmilevitch et al. 2004, Krapp et al. 2011). Thus, RFNR may play a minor role in N reduction in roots grown with nitrate. Ammonium addition to *Arabidopsis* roots induced *NADH-GOGAT* rather than *Fd-GOGAT* expression in a concentration-dependent manner (Konishi et al. 2014). Moreover, analyses with loss-of-function mutants have suggested that NADH-GOGAT is the major enzyme converting ammonium-derived glutamine to glutamate in roots (Lancien et al. 2002, Konishi et al. 2014). It is therefore doubtful that RFNR supports nitrogen assimilation by furnishing Fd-GOGAT with reduced Fd in roots grown with ammonium.

Recently, nitrite has been attracting attention as the third inorganic N source (Kotur et al. 2013). Nitrite availability varies in the soil worldwide depending on the balance between nitrification and denitrification (Samater et al. 1998, Riley et al. 2001, Shen et al. 2003). Although nitrite concentrations in the soil are generally low compared with nitrate and ammonium, a few hundred μM of nitrite have been detected in some soils (Jones and Schwab 1993, López Pasquali et al. 2007). Nitrite can be taken up via different pathways in *A. thaliana* (Kotur et al. 2013). One is mediated via active transporters including high-affinity nitrate transporter 2 (NRT2), and another is simple diffusion of nitrous acid under low pH. It is noteworthy that micromolar concentrations of nitrite act as a signal to rapidly alter a genome-wide expression of numerous transcripts in *A. thaliana* (Wang et al. 2007). The existence of functional machineries for nitrite uptake and signaling suggests that nitrite could be an important N source for plants in the field. Nitrite must be reduced immediately after its uptake, because of its high toxicity to plants. In fact, *AtRFNRs* and *NIR* can be induced by application of only 5 μM nitrite within 20

minutes (Wang et al. 2007). Therefore, we verified the hypothesis that RFNR could have a major role in reducing environmental nitrite as N source using *A. thaliana* seedlings of wild type (Col) and loss-of-function mutants of *RFNR*. Our results strongly suggest that AtRFNR2 is essential for reduction and detoxification of nitrite absorbed by roots to avoid accumulation of nitrite and the resultant defects in plant growth.

Results

Identification of T-DNA insertion mutants of RFNR1 and RFNR2

One T-DNA insertion allele for *RFNR1* (SALK_085009; *rfnr1*) and two independent alleles for *RFNR2* (SAIL_527_G10.V1; *rfnr2-1*, SALK_133654; *rfnr2-2*) were obtained from the European Arabidopsis Stock Centre (Fig. 1A). *rfnr1* and *rfnr2-1* have T-DNA insertions in the second exon and in the first intron, respectively. An insertion of T-DNA in *rfnr2-2* extends from the fourth exon to the fourth intron. We checked mRNA levels of full-length *RFNRs* in roots of these lines with reverse transcription PCR (RT-PCR) (Fig. 1B, Supplementary Fig. S1A). In *rfnr1* and *rfnr2-2*, there was no transcript signal from the corresponding *RFNR* genes (Fig. 1B). On the other hand, lower amounts of signals were detected in *rfnr2-1* than Col (Supplementary Fig. S1A). A quantitative reverse transcription PCR (Q-PCR) analysis also revealed that transcript levels of *RFNR2* in *rfnr2-1* accounted for about 18-25% of the transcript amount in Col roots (Supplementary Fig. S1B). To determine protein content of RFNRs, we conducted western analysis with the polyclonal antibody raised against a recombinant maize RFNR (Onda et al. 2000). Two independent signals were observed in Col, where the upper and lower bands correspond to RFNR1 and RFNR2, respectively (Hanke et al. 2005). In *rfnr1*, no upper signal was detected, whereas, in *rfnr2-1* and *rfnr2-2*, the lower signal was absent (Fig. 1C, Supplementary S1C). We concluded that *rfnr1* and *rfnr2-2* are knockout mutants and that *rfnr2-1* is a knockdown mutant.

Expression of RFNR1 and RFNR2 under different N growth conditions

To determine steady-state transcript levels of *RFNR1* and *RFNR2* under

199 different N sources, we conducted Q-PCR analysis using Col grown with 0.2 mM of
200 nitrate (NA), nitrite (NI) or ammonium (A) as the sole N source for seven days (Fig. 2A).
201 This N concentration is within the conceivable range in the field (Miller et al. 2007, Kotur
202 et al. 2013), and was sufficient to grow plants without causing N depletion (see protein
203 contents in plants in Fig. 4E). Irrespective of N source, both *RFNRs* were expressed
204 predominantly in roots (Fig. 2A), where the copy numbers of *RFNR2* mRNA were more
205 than ten times those of *RFNR1*. In the roots of Col grown with nitrite, a western analysis
206 also showed that RFNR2 had stronger signals than RFNR1 (Fig. 1C). The transcript levels
207 of *RFNR1* were similar among N conditions both in shoots and roots, whereas those of
208 *RFNR2* attained the maximum level in the roots grown with nitrite.
209 Nitrate and nitrite application can induce expression of a large number of genes
210 in tens of minutes (Wang et al. 2003, Wang et al. 2007, Patterson et al. 2010). To analyze
211 the short-term N responses, we grew seedlings for seven days under ammonium
212 conditions and transferred them into fresh media containing nitrate, nitrite or ammonium
213 as the sole N source. *RFNR2* expression levels in roots were compared before and after a
214 30 minute incubation with each N source (Fig. 2B). *RFNR2* was significantly induced by
215 nitrite addition, but not by nitrate or ammonium. In the present study, we focused on
216 RFNR2 as the major isoform responding to nitrite-supplied conditions.
217 To monitor a tissue-specific pattern of transcriptional activity for *RFNR2*, we
218 generated transgenic plants with β-glucuronidase (GUS) fused to the region between –
219 879 and +24 bp from the first ATG codon of *RFNR2* (For details, see Materials and
220 methods). The T_3 homozygous transgenic plants were grown for five days under nitrate

221 or nitrite, and blue GUS signals were observed with a stereoscopic microscope (Fig. 2C)
222 and an optical microscope (Fig. 2D, E). Under both N sources, the signals were localized
223 predominantly in roots, consistent with the Q-PCR observations (Fig. 2A, C). Basal
224 regions of primary roots had stronger signals than root tips (Fig. 2C). In the middle region
225 of the primary root, vascular bundles were remarkably stained, although the outer layer
226 of cells also showed weaker GUS signals (Fig. 2D). Strong signals were also observed in
227 the columella cells of root tips (Fig. 2E). Overall, the signal intensities of GUS were
228 higher under nitrite than nitrate (Fig. 2C-E), which also corresponded to the tendency
229 observed with Q-PCR (Fig. 2A, B). Both transcript levels of authentic *RFNR2* and
230 heterologous *GUS* driven by the *RFNR2* promoter were higher in 5-day-old roots under
231 nitrite (Fig. 2F), suggesting that the nitrite induction of *RFNR2* is under transcriptional
232 control.
233
234 *Root growth of rfnr2 mutants on different N sources*
235 Next, we compared root growth between Col and *rfnr2* mutants to elucidate
236 whether RFNR2 could contribute to nitrite reduction (Fig. 3, Supplementary Fig. S1D-
237 F). In Col, the length of primary roots was slightly, but significantly, longer under nitrate
238 growth conditions than with nitrite or ammonium (Fig. 3A, B, Supplementary Fig. S1D,
239 E). Primary root growth of *rfnr2-2* decreased relative to Col under nitrite growth
240 conditions, whereas, under nitrate or ammonium condition, no significant difference was
241 observed. Also, in *rfnr2-1*, primary root length was shorter under nitrite, but not under
242 nitrate. The length of lateral roots was also longest in Col supplied with nitrate, followed

243 in order by nitrite and ammonium (Fig. 3A, C, Supplementary Fig. S1D, F). Relative to
244 Col, *rfnr2-2* showed remarkably stunted growth of lateral roots under nitrite growth
245 conditions, although the mutant also had a slight decrease in lateral root length under
246 nitrate conditions (Fig. 3C). In *rfnr2-1*, however, no significant decrease in lateral root
247 length was observed (Supplementary Fig. S1F).

248 We then investigated root growth in the knockout mutant, *rfnr2-2*, in detail. To
249 determine the effective concentration of nitrite that results in primary root defects in
250 *rfnr2-2*, we analyzed the concentration-dependence of primary root elongation on nitrate
251 or nitrite at 0, 0.04, 0.2 and 1 mM (Fig. 3D). Little difference in primary root length was
252 observed between Col and *rfnr2-2* under nitrate growth conditions at any concentration.
253 By contrast, nitrite caused primary root elongation defects in *rfnr2-2* plants at 0.04, 0.2
254 and 1 mM. The extent of this defect in root growth increased with the nitrite
255 concentration. It should be noted that primary root lengths in *rfnr2-2* were shorter under
256 nitrite than under no N condition, suggesting that the stunted root phenotype is primarily
257 due to a detrimental effect of nitrite on root growth, rather than an inability to assimilate
258 N in the roots.

259 A time-course analysis revealed that, on nitrite supply, daily primary root
260 elongation in *rfnr2-2* was severely suppressed at early stages of development (4-6 d), and
261 that the suppression tended to be mitigated at later stages (7-9 d) (Fig. 3E).

262 To validate whether the root growth defects of *rfnr2-2* plants grown on nitrite
263 persist, we transferred 4-day-old seedlings grown on either nitrate or nitrite to fresh
264 medium containing different N sources. The seedlings were grown for three further days,

and their primary root elongation during the period after transfer was determined (Fig. 3F). Irrespective of the N source before the transfer, the *rfnr2-2* transferred to nitrite condition showed stunted primary root growth. On the other hand, the transfer from nitrite to nitrate conditions restored the rate of primary root elongation. These data suggest that the defective phenotype of the mutant is reversible.

Exploring the causes of root growth defects in rfnr2

If RFNR2 contributes to nitrite reduction in roots, its deficiency should cause nitrite accumulation therein. To confirm this, we measured nitrite concentrations in roots of 7-day-old plants grown under nitrate or nitrite (Fig. 4A). Under nitrite conditions, more than 100 nmol g fresh weight^{-1} of nitrite was determined in *rfnr2-2* roots, whereas nitrite was not significantly detected in Col roots. Nitrite also accumulated in the roots of *rfnr2-1*, although the extent was less than in *rfnr2-2* (Supplementary Fig. S1G). In roots of plants grown with nitrate, no significant amount of nitrite was detected in either Col or *rfnr2-2* (Fig. 4A), indicating that any contribution of RFNR2 to N assimilation in Arabidopsis is redundant. Excess accumulation of nitrite is frequently accompanied by nitric oxide (NO) biosynthesis via a side reaction catalyzed by nitrate reductase (NR) (Rockel et al. 2002, Wang et al. 2007), which may inhibit primary root growth (Fernández-Marcos et al. 2012). Thus, we checked whether a NO scavenger could restore primary root growth in *rfnr2-2* roots grown with nitrite (Fig. 4B). However, application of 200 µM of carboxy-PTIO did not affect the phenotype in *rfnr2-2*. Likewise, the transcript level of an NO-inducible marker gene, *AOX1a* (Huang et al. 2002), was

287 unaffected by *RFNR2* deficiency (Fig. 4C). Furthermore, we could not detect NR activity
288 in nitrite-grown Col roots, whilst, in the shoots, 8.27 ± 1.53 nmol g FW^{-1} min^{-1} of NR
289 activity was measured (Fig. 4D). Taken together, the data contradict any contribution of
290 NO to root growth defects in the *RFNR2* mutants.

291 Severe N depletion decreases primary root growth in *A. thaliana* (Araya et al.
292 2014), providing another possible explanation for the *rfnr2* phenotype: *RFNR2* deficiency
293 may deplete total N assimilation when nitrite is supplied as the sole N source. We
294 therefore measured protein amounts in 7-day-old seedlings of Col and *rfnr2-2* (Fig. 4E),
295 but could not observe any significant decrease in protein content of *rfnr2-2* seedlings,
296 indicating that NiR activity in the leaves, supported by photosynthesis, is sufficient for N
297 assimilation. Moreover, additional application of 0.2 mM nitrate or 0.2 mM ammonium
298 to 0.2 mM nitrite (i.e. 0.4 mM N included in the media) did not restore the wild type root
299 phenotype in *rfnr2-2* (Fig. 4F, G). In addition, as demonstrated in Fig.3D, primary root
300 lengths in *rfnr2-2* were even shorter with nitrite than under no N growth conditions. These
301 observations suggest that toxicity of nitrite *per se* could suppress root growth in *rfnr2-2*,
302 and that the impairment of root growth is not due to N deprivation.

303

304 *Identification of genes acting with RFNR2 in nitrite detoxification*

305 To provide reducing power for efficient nitrite reduction in roots, NIR, RFNR,
306 Fd and oxPPP would have to respond to nitrite concomitantly (see Introduction). To
307 identify a set of additional, specifically relevant genes, we surveyed genes co-expressed
308 with *RFNR2* using the ATTED II program (Obayashi et al. 2014). Supplementary Table

S1 shows a list of genes within the ranking's top ten. This includes one *NIR* (*NIR*; At2g15620), one root type *FD* (*FD3*; At2g27510) and one *FNR* (*RFNR1*; At4g05390). In the oxPPP, two *GLUCOSE-6-PHOSPHATE DEHYDROGENASEs* (*G6PD2;* At5g13110, *G6PD3*; At1g24280), two putative *6-PHOSPHOGLUCONATE DEHYDROGENASEs* (At1g64190, At5g41670) and one *TRANSALDOLASE* (*TRA2*; At5g13420) were identified. We analyzed whether *NIR*, *FD3*, *RFNR1*, *G6PD2*, *G6PD3*, *At1g64190* and *At5g41670* could respond to different N sources in the same way as *RFNR2* (Fig. 5A, B). Under steady-state growth conditions, all these genes were expressed predominantly in roots, and their expression levels attained the maximum in roots grown with nitrite (Fig. 5A). On the other hand, expression of the reference gene *At4g34270* (Hong et al. 2010) was not significantly different between N sources in shoots or roots (Fig. 5A). Short-term analysis also revealed that induction of the above genes was consistently strongest following nitrite application, whereas expression of *At4g34270* was not significantly changed (Fig. 5B). This expression response pattern is similar to that of *RFNR2* (Fig. 2A, B), suggesting that the products of these genes act cooperatively with RFNR2 to form an electron supply system for nitrite reduction in roots. If this hypothesis is correct, nitrite induced expression of these genes would be enhanced in the *RFNR2* mutants as compensation. As expected, the steady-state transcript levels were higher in *rfnr2-2* roots under nitrite growth conditions (Fig. 5C), while *At4g34270* expression was affected little by *RFNR2* deficiency. A similar tendency was found in *rfnr2-1*, although the extent of compensation was less than in *rfnr2-2* (Supplementary Fig. S1H).

Verifying the role of RFNR2 with nitrate or ammonium as N sources

We found little difference in root growth between Col and *RFNR2* mutants under nitrate or ammonium growth conditions (Fig. 3, Supplementary Fig. S1D, E). This means that RFNR2 may only play a minor role in N assimilation from these N sources, as mentioned in the Introduction. In short, we assume that in *A. thaliana*, nitrate reduction and the subsequent Fd-dependent steps occur mainly in shoots, and that ammonium absorbed by the roots is assimilated into glutamine by GS in the roots, followed by its conversion to glutamate mainly by NADH-GOGAT.

If nitrate was reduced predominantly in shoots, NR activity would be higher in shoots than roots. Indeed, in seedlings grown with nitrate, an abundant activity of NR was detected in shoots, but no significant activity was detected in roots (Fig. 6A, for comparison, see Yu et al. 1998, Konishi and Yanagisawa 2011). In a NR double mutant (*nr*) grown in the presence of nitrate, more nitrate was accumulated in shoots relative to Col, but not in roots (Fig. 6B), confirming that nitrate reduction occurs mainly in shoots *in vivo*. Furthermore, in Figure 4A, *RFNR2* deficiency did not affect nitrite concentrations in roots under nitrate growth conditions, suggesting that nitrite was scarcely produced in the roots grown with nitrate.

GLN1;2 is an ammonium-inducible isoform of GS expressed in the root vasculature (Ishiyama et al. 2004, Konishi et al. 2014, Guan et al. 2015). Our Q-PCR analysis revealed that *GLN1;2* was expressed predominantly in roots, and attained maximum expression levels under ammonium growth conditions (Supplementary Fig. S2A). On the other hand, transcripts of *GLN2*, the plastidic isoform of GS, were much

353 higher in shoots than roots. Total GS activities are almost comparable between shoots and
354 roots (Supplementary Fig. S2B). In roots, the highest activity was observed under
355 ammonium growth conditions, followed by nitrite and then nitrate conditions,
356 corresponding to the expression pattern of *GLN1;2* (Supplementary Fig. S2A, B). A
357 knockout of *GLN1;2* (*gln1;2*, Lothier et al. 2011) decreased root GS activity by ca. 35%
358 of Col (Fig. 6C). More ammonium was accumulated in the *gln1;2* roots grown with
359 ammonium than Col (Fig. 6D). Furthermore, *gln1;2* showed impaired lateral root growth
360 under ammonium (Supplementary Fig. S2C). These observations indicate that a
361 significant portion of ammonium absorbed by roots is normally assimilated in the root.
362 Following ammonium incorporation into glutamine, the subsequent conversion of
363 glutamine to glutamate can be catalyzed by Fd-GOGAT (*GLU1*, *GLU2*) or NADH-
364 GOGAT (*GLT*). Q-PCR analysis showed that, of these three genes, *GLU2* and *GLT* were
365 predominantly expressed in roots (Supplementary Fig. S2D). If RFNR2 contributes to
366 glutamate biosynthesis under ammonium growth conditions, the contents of glutamine
367 and glutamate in the roots would be expected to change on *RFNR2* deficiency. The results,
368 however, show that there is no significant difference in either amino acid between Col
369 and *rfnr2-2* (Fig. 6E). Moreover, no compensatory induction of *RFNR1*, *FD3*, *G6PD3*,
370 *At5g41670*, *GLT* or *GLU2* expression occurred in *rfnr2-2* grown with ammonium
371 (Supplementary Fig. S2E). These results suggest that RFNR2 does not make a significant
372 contribution to glutamate biosynthesis under ammonium growth conditions. Taken
373 together, we conclude that RFNR2 has a significant role in N reduction/assimilation of
374 nitrite, rather than nitrate or ammonium.

Discussion

Plants use nitrate and ammonium as major N sources (Kiba and Krapp 2016). Currently, these are recognized as not only substrates for protein synthesis but also signals that alter gene expression and root morphology (Remans et al. 2006, Lima et al. 2010, Patterson et al. 2010). To date, the components for their transport and signaling have been comprehensively identified and characterized (Krapp et al. 2015). On the other hand, far less information about nitrite is available, although measurable amounts of nitrite are often present in the soil and can accumulate to high levels depending on pH (Shen et al. 2003, Kotur et al. 2013). Nitrite is actively taken up by specific transport systems and used for N assimilation (Kotur et al. 2013). Plants can sense exogenous nitrite at micromolar concentrations, and respond by altering their transcriptome (Wang et al. 2007). There is no doubt that nitrite is a third inorganic N source worthy of attention. NiR is the sole enzyme for nitrite reduction and is completely dependent on the reduced form of ferredoxin as an electron donor. In *NIR* antisense tobacco plants, growth is suppressed with accompanying accumulation of nitrite to extremely high concentrations (Morot-Gaudry-Talarmain et al. 2002). Our results suggest that in *rfnr2* mutants NiR can not fulfill its physiological role in roots due to a limitation in electron supply.

The data presented here indicate that in Arabidopsis, both NO_3 and NH_4, but not NO_2, are primarily transported to the shoot for assimilation. If such a mechanism were also applied to NO_2, the plant would be subject to severe toxic effects. To avoid this, NO_2 assimilation depends on an effective electron supply to NiR by RFNR in the root, in

order to reduce NO_2 to NH_4 before transport to the leaf.

Here we provide strong evidence supporting the hypothesis that *in vivo* the flux rate of nitrite reduction is decreased in the *RFNR2* mutants as the system for supplying reduced Fd to NiR is disrupted. However, testing this hypothesis directly is experimentally problematic using the conventional method of assaying NiR activity. In this method, maximum activity of NiR is measured with an excess amounts of electron donors. Thus, it would not reflect *in vivo* flux rate of nitrite reduction, and any defect in NiR reduction due to impaired electron supply would not be detected. It is therefore a research priority to develop a new method for quantitative evaluation of the flux rate in the future.

Primary root growth of two *RFNR2* mutants decreased relative to Col under nitrite growth conditions, whereas only *rfnr2-2* showed the stunted growth of lateral roots under nitrite. This phenotypic discrepancy may reflect the extent of genetic defects (i.e. knockout in *rfnr2-2*, knockdown in *rfnr2-1*). We concluded that *RFNR2* deficiency impacts on primary root growth when nitrite is supplied as the N source.

Given that nitrite is toxic, its conversion to organic N results in detoxification. Since nitrite reduction occurs only in plastids, this toxic nitrite should be promptly transported into plastids before its reduction. In *A. thaliana*, specific transporters for nitrite uptake into plastids have been identified as *NITR2;1* and *NITR2;2* (Maeda et al. 2014). The promoter-directed GUS signal of *NITR2;2* was detected exclusively in roots. An *in silico* survey for the genes co-expressed with *RFNR2* found that *NITR2;2* was ranked 13th (Obayashi et al. 2014). NITR2;2 may therefore be important for the

419 immediate reduction of nitrite taken up from the soil.

420 Our expression analysis confirmed that *AtRFNR1* was expressed at a lower
421 level than *AtRFNR2*, and AtRFNR1 is a minor form (Fig. 1C, 2A). It is possible that
422 RFNR1 has some redundant function with RFNR2 in roots, because *RFNR1* showed a
423 similar expression pattern to *RFNR2* in response to different N sources (Fig. 5B) and
424 *RFNR1* was induced in *rfnr2-2* in a compensatory manner (Fig. 5C). Interestingly, the
425 suppression of primary root elongation in *rfnr2-2* was mitigated at its later growth stages
426 under nitrite growth conditions (Fig. 3E), indicating that *RFNR1* might partly alleviate
427 nitrite accumulation and its toxicity in *rfnr2-2*, although the compensation was not
428 sufficient to completely restore the root growth (Fig. 3). On the other hand, root growth
429 of a *RFNR1* knockout mutant was not impaired under nitrite growth conditions
430 (Supplementary Fig. S3A-C). The contribution of RFNR1 to reduction of nitrite absorbed
431 by roots is therefore probably limited.

432 The genes coexpressed with *RFNR2* in Figure 5 have all been identified as both
433 nitrate- and nitrite-inducible genes (Supplemental Data in Wang et al. 2007). In this case,
434 we observed that nitrite induced much stronger effects on gene expression than nitrate
435 (Fig. 5A, B). A uniform response of the genes indicates strict control of expression by a
436 single mechanism that originates with nitrite perception. Both expression of *NIR* and
437 *NITR2;2* are under the control of the NIN-like protein (NLP) family of transcription
438 factors, responding to nitrate *per se* (Konishi and Yanagisawa 2013, Maeda et al. 2014).
439 A mutation of the nitrate sensor *CHL1/NRT1.1/NPF6.3* suppressed nitrate induction of
440 genes related to nitrite detoxification examined in Figure 5 (Supplemental Data in Wang

et al. 2009). Considering that over one-half of nitrite-responding genes overlap with nitrate-responding genes (Wang et al. 2007) and that the molecular structure of nitrate and nitrite is similar, it is possible that the same components could be involved in both nitrate signaling and the nitrite induction of these genes.

In *A. thaliana*, chloroplasts purified from *LFNR1* knockout plants had enhanced activities of nitrite reduction compared with those from Col (Hanke et al. 2008). This implies a competition for reduced Fd between LFNR and NIR. Bloom et al. (2010) have demonstrated that, in leaves, the conversion from nitrate to ammonium is suppressed under elevated CO_2 with nitrate as an N source. This suggests that increased demand on NADPH for CO_2 assimilation in the Calvin Benson cycle could deplete the reduced leaf Fd available for NIR. Thus, some leaf localized Fd-dependent enzymatic reactions may be limited by electron supply under high CO_2, which in turn, could necessitate a greater contribution of root localized Fd-dependent reactions to bioassimilatory and biosynthetic processes. Enhanced CO_2 assimilation under high CO_2 has been shown to increase carbon partitioning to roots (Duan et al. 2014), providing more sugar for NADPH production in the oxPPP. Reduction of root Fd by RFNR is a future research target worthy of attention in the context of increasing CO_2 concentrations in the atmosphere.

Materials and Methods

Plant materials and growth conditions

Arabidopsis thaliana (L.) Heynh. accession Col and mutants *rfnr1*-KO (SALK_085009), *rfnr2*-KO (SALK_133654), *rfnr2*-KD (SAIL_527_G10), *gln1;2*-KO (SALK_102291, Lothier et al. 2011) and *nia1-1nia2-5* (*nr*), a *NITRATE REDUCTASE* double mutant (Wilkinson and Crawford 1993) were used in our experiments. The seeds were purchased from the European Arabidopsis Stock Centre. After surface sterilization, 10 seeds were sown on plastic Petri dishes (length 140 mm, width 100 mm, depth 20 mm; Eiken Kagaku, Tokyo, Japan) containing 50 ml of half-strength Murashige and Skoog-macro- and micro-nutrient salts (except for N) with 0.05% (w/v) MES-H_2O, 1% (w/v) sucrose (Murashige and Skoog 1962). For the media containing 0.2 mM of nitrate (NA), nitrite (NI) or ammonium (A), 0.2 mM KNO_3 and 1.8 mM KCl, 0.2 mM KNO_2 and 1.8 mM KCl or 0.2

mM NH_4Cl and 2 mM KCl were added, respectively. The media were solidified with 0.5% (w/v) gerangum, and pH of the media was adjusted to 6.15 with KOH. After sowing, the plates were kept at 4°C in the dark for three days. Plants were grown in a vertical position on plastic dishes under a photosynthetic photon flux density of 100–120 μmol m^{-2} s^{-1} (16 h light/8 h dark cycle) at 23°C. Ten seeds per plate were sown in all experiments. For comparisons between Col and mutants, five seeds of each line were placed on the same plate, if not specified. Further details are given in the Results and figure legends.

Root growth analysis

For analysis of root growth, 7-day-old plants were harvested and scanned at 300 dpi resolution for measurement of root length according to Hachiya et al. (2014). The root architecture was traced using Photoshop Elements 11 (Adobe Systems), and the lengths of primary and lateral roots were measured from traced images using ImageJ software (ver.1.47).

Preparation for segmented plates

A localized addition of nitrate or nitrite to plants was accomplished using segmented plates where two patches were separated by an air gap (Remans et al. 2006). For preparation of the segmented plate, basic nutrient media (as described above) containing no N sources were solidified. The narrow gel split was eliminated with sterile razors and forceps to create an air gap. Subsequently, concentrated potassium nitrate or

potassium nitrite were placed and spread on each patch of the media. To allow homogenous diffusion of the N sources, the plated were prepared more than 48 h before the experiments. Three 4-day-old Col and *rfnr2-2* plants of each line grown on 0.2 mM of ammonium medium were transferred onto the segmented plates. It should be noted that shoots and roots were in contact with only the upper and lower patches, respectively. The plants were grown for a further three days, and elongation of the primary root was measured as described above.

Extraction of total RNA, reverse transcription and real-time PCR

For purification of total RNA, shoots or roots were harvested, immediately frozen with liquid N_2 and stored at −80°C before use. All samples per plate were regarded as one biological replicate. Frozen samples were ground with a TissueLyser II (QIAGEN, Hilden, Germany) using 5 mm zirconia beads. Total RNA was extracted using RNeasy plant mini kit (QIAGEN) according to the manufacturer's instructions with on-column DNase digestion. Reverse transcription was performed with a ReverTra Ace qPCR RT Master Mix (Toyobo Life Science, Tokyo, Japan) according to the manufacturer's instructions. The synthesized cDNA was diluted 10-fold with distilled water for real-time PCR.

Transcript levels were measured using a StepOnePlus Real-Time PCR System (ThermoFisher Scientific, Waltham, MA, USA). cDNA (2 µl) was amplified in the presence of 10 µl of KAPA SYBR FAST qPCR Kit (Nippon Genetics Co., Ltd., Tokyo, Japan), 0.5 µl of specific primers (0.2 µM final concentration) and 7.5 µl sterilized water.

529 Transcript levels were quantified using absolute or relative standard curve with *ACTIN3*
530 as the internal standard. Plasmid DNA containing the corresponding cDNAs or total
531 cDNAs were used as templates to generate standard curves. Primer sequences used for
532 the experiments are shown in Supplemental Table S2. Primers were designed with the
533 NCBI/Primer-BLAST program.
534
535 *Western analysis of RFNR proteins*
536 Roots were harvested, immediately frozen with liquid N_2 and stored at −80°C
537 before use. All samples per two plates were regarded as one biological replicate. Frozen
538 samples were ground with a TissueLyser II (QIAGEN) using 5 mm zirconia beads. Total
539 proteins were extracted with 10 volumes of sample buffer (NuPAGE LDS Sample buffer
540 and NuPAGE Reducing Agent, ThermoFisher Scientific) followed by incubation at 95˚C
541 for 5 min. The extracts were centrifuged at 20,400 *g* at room temperature for 10 min. 10
542 µl of the supernatant was subjected to SDS-PAGE in a 15% (w/v) gel and transferred to
543 a PVDF membrane (Immobilon-P, Merck Millipore, Darmstadt, Germany) at 2 mA cm^{-2}
544 for 1.5 h in transfer buffer (NuPAGE Transfer Buffer, ThermoFisher Scientific). The
545 membrane was incubated in blocking buffer containing ECL Prime Blocking Agent (GE
546 Healthcare, Little Chalfont, UK), 0.02% Tween-20, 20 mM Tris-HCl, pH 7.4, 140 mM
547 NaCl for 1 h, and reacted with a 1/50000 dilution of the polyclonal antibody raised against
548 maize RFNR overnight (Onda et al. 2000). After rinsing, the antigen-antibody complex
549 was detected by 1/50000 dilution of horseradish peroxidase (HRP)-conjugated with goat
550 antibody against rabbit IgG (NA935, GE Healthcare) and visualized by chemiluminescent

551 detection (ECL Prime, GE Healthcare) using ImageQuant LAS 4010 (GE Healthcare).

552

553 *Determination of nitrate, nitrite, ammonium, glutamine, glutamate and protein*

554 Nitrate was extracted and determined according to Hachiya et al. (2012) with
555 slight modifications. Shoots or roots were harvested and dried at 80˚C before use. All
556 samples per plate were regarded as one biological replicate. Nitrate was extracted with
557 10 volumes of water at 100˚C for 10 min. 10 µl of supernatant was mixed with 40 µl of
558 reaction reagent (50 mg salicylic acid per one ml concentrated sulfuric acid), and the
559 mixture was incubated at room temperature for 20 min. For the mock treatment, 40 µl of
560 concentrated sulfuric acid only was added to 10 µl of supernatant. After an addition of 1
561 ml of NaOH to the mixture, absorbance at 410 nm was scanned. Nitrate content of the
562 supernatant was calculated based on standard curve with dilution series of potassium
563 nitrate.

564 For nitrite determination, roots were harvested, immediately frozen with liquid
565 N_2 and stored at −80°C before use. All samples per five plates were regarded as one
566 biological replicate. Frozen samples were ground with a TissueLyser II (QIAGEN) using
567 5 mm zirconia beads. Nitrite was extracted with 5 volumes of extraction buffer (50 mM
568 Hepes-KOH, pH7.6, 1 mM EDTA, 7 mM cysteine). The extracts were centrifuged at
569 20,400 *g* at 4°C for 10 min. The supernatant was mixed with equal volumes of 1% (w/v)
570 sulfanilamide solution in 1N HCl and 0.02% (w/v) N-1-Naphthylethylenediamine
571 dihydrochloride solution in H_2O. For detection of the nonspecific background, 1% (w/v)
572 sulfanilamide solution in 1N HCl was replaced by 1N HCl. The mixture was incubated at

573 room temperature for 15 min followed by scanning absorbance at 540 nm. Nitrite content
574 of the supernatant was calculated based on standard curve with dilution series of
575 potassium nitrite by subtracting the background values from the total values.

576 For ammonium determination, roots were harvested, immediately frozen with
577 liquid N_2 and stored at −80°C before use. All samples per plate were regarded as one
578 biological replicate. Ammonium was extracted and determined according to Bräutigam
579 et al. (2007) with slight modifications. Frozen samples were ground with a TissueLyser
580 II (QIAGEN) using 5 mm zirconia beads. 1 ml of 0.1 N HCl and 500 µl of chloroform
581 were added to the frozen powder. The mixture was rotated for 15 min at 4˚C followed by
582 centrifugation at 12,000 *g* at 8°C for 10 min. The aqueous phase was further purified by
583 acid-washed activated charcoal (No. 035-18081; Wako, Osaka, Japan). Ammonium
584 content of the supernatant was spectroscopically determined using an ammonia test kit
585 (No. 277-14401, Wako) according to the manufacturer's instructions.

586 For determination of glutamine and glutamate, roots were harvested,
587 immediately frozen with liquid N_2 and stored at −80°C before use. All samples per five
588 plates were regarded as one biological replicate. Glutamine and glutamate were extracted
589 and determined according to Kamada-Nobusada et al. (2013). Frozen samples were
590 ground with a TissueLyser II (QIAGEN) using 5 mm zirconia beads. The powder was
591 mixed with 10 volumes of 10 mM HCl containing 0.2 mM methionine sulfone as an
592 internal control. The homogenate was centrifuged at 20400 *g* at 4˚C for 5 min, and the
593 supernatant was filtered through Ultrafree-MC filters (No. UFC30GV00, Merck
594 Millipore). Amino acid contents in the resulting filtrate were determined using Pico-Tag

595 (Waters Corporation, Milford, MA, USA) with an HPLC System (Waters Alliance 2695
596 HPLC system/2475) according to the manufacturer's instructions.
597 Total protein was extracted as described above. 10 µl of the extracts were
598 suspended into 500 µl of H_2O, after which 100 µl of 0.15 % (w/v) sodium deoxycholate
599 aqueous solution was added, and the mixture was incubated at room temperature for 10
600 min. Subsequent addition of 100 µl of 72% (v/v) trichloroacetic acid was followed by
601 incubation at room temperature for 15 min. The mixture was centrifuged at 20,400 *g* at
602 room temperature for 10 min, and the precipitates were dried at room temperature and
603 used for protein determination by a BCA method (Takara BCA Protein Assay Kit No.
604 T9300A, Takara Bio Inc., Otsu, Japan) according to the manufacturer's instructions.
605
606 *Determination of activities of nitrate reductase and glutamine synthetase*
607 NR activity was determined according to Konishi and Yanagisawa (2011).
608 Shoots or roots were harvested, immediately frozen with liquid N_2 and stored at −80°C
609 before use. All samples per two plates were regarded as one biological replicate. Frozen
610 samples were ground with a TissueLyser II (QIAGEN) using 5 mm zirconia beads. The
611 powder was mixed with 5 volumes of extraction buffer (50 mM Hepes-KOH, pH7.6, 1
612 mM EDTA, 7 mM cysteine). The extracts were centrifuged at 20,400 *g* at 4°C for 10 min.
613 25 µl of the supernatant was added to 75 µl of assay buffer (50 mM Hepes-KOH, pH7.6,
614 100 µM NADH, 2 mM EDTA, 5 mM KNO_3). After incubation at 30°C for 15 min, nitrite
615 produced was determined as mentioned above.
616 GS activity was determined as the ADP-dependent conversion rate of L-

617 glutamine to γ-glutamylhydroxamate according to Taira et al. (2004) and Li et al. (2012)
618 with slight modifications. Shoots or roots were harvested, immediately frozen with liquid
619 N_2 and stored at −80°C before use. All samples per two plates were regarded as one
620 biological replicate. Frozen samples were ground with a TissueLyser II (QIAGEN) using
621 5 mm zirconia beads. The powder was mixed with 10 volumes of extraction buffer (100
622 mM Tris-HCl, pH7.5, 1% (w/v) PVP-40, 1 mM EDTA, 1 mM $MnCl_2$, 0.5% (v/v) β-
623 mercaptoethanol, 0.1 mM APMSF). The extracts were centrifuged at 12,000 *g* at 4°C for
624 10 min. 45 μl of assay buffer (40 mM imidazole-HCl, pH 7.0, 20 mM sodium arsenate,
625 0.5 mM ADP, 3 mM $MnCl_2$, 60 mM NH_2OH, 30 mM L-glutamine) was added to 5μl of
626 the supernatant, and the mixture was incubated at 30°C for 15 min. Reactions were
627 stopped by adding 30 μl of $FeCl_3$-TCA-HCl solution (2.6% $FeCl_3 \cdot 6H_2O$, 4%
628 trichloroacetic acid in 1N HCl). The products were measured by absorbance at 540 nm.
629
630 *Construction of ProRFNR2:GUS fusions*
631 The putative promoter region (–879 to +24 bp from the first ATG codon) was
632 amplified from *Arabidopsis* genomic DNA using PrimeSTAR GXL DNA Polymerase
633 (Takara Bio Inc.) and specific primers (see Supplemental Table 2). PCR products were
634 cloned into pENTR using pENTR/D-TOPO Cloning Kit (ThermoFisher Scientific)
635 according to the manufacturer's instructions, sequenced, and subcloned into pBA002a-
636 GW-GUS (Kiba et al. 2007) by LR reaction. The binary vector was transformed into
637 *Agrobacterium* strain EHA101. Transformants were selected on LB medium containing
638 100 mg L^{-1} spectinomycin and positive clones were recovered. *Arabidopsis* plants

accession Col was transformed by the floral dip method (Clough and Bent 1998). Transgenic seedlings were isolated on Murashige and Skoog medium containing 1% sucrose and 5 mg L^{-1} bialaphos sodium salt. Segregation ratios were analyzed to select plants with one copy of T-DNA and to isolate homozygous plants. T3-homozygous plants were used for experiments.

GUS Staining

Histochemical GUS staining was performed according to Jefferson (1987) with slight modifications. Plants were incubated in 90% (v/v) acetone solution on ice for 15 min, and submerged into assay buffer (100 mM sodium phosphate, pH 7.4, 10 mM EDTA, 5 mM ferro/ferricyanide, 0.1% (v/v) Triton X-100, 0.5 mg mL^{-1} X-Gluc), followed by vacuum infiltration at room temperature for 15 min. Plants were incubated in the dark at 37 ˚C for 4.5 h. The stained plants were washed with 70 % (v/v) ethanol and bleached with 6:1 (v/v) ethanol : acetic acid. The samples were mounted with chloral hydrate solution (8:1:2 (w/v/v) chloral hydrate : glycerol : H_2O) and observed using a stereoscopic microscope (Olympus SZX12, Olympus, Tokyo, Japan) and an optical microscope (Olympus BX53).

Statistical analysis

All statistical analyses were conducted using the R software package (ver. 2.15.3). Details of analyses are given in the Results and in table and figure legends.

Funding

This work was supported by RIKEN Special Postdoctoral Researchers (SPDR) fellowship to T.H..

Disclosures

Conflicts of interest: No conflicts of interest declared.

Acknowledgements

We are grateful to Prof. Crawford for the kind gifts of the mutant seeds. Prof. Terashima, Prof. Noguchi and Dr. Kiba are thanked for important advice and for making available the pBA002a-GW-GUS vector. We thank Ms. Akiko Suzuki for her technical assistance.

683

684

685

686

687

688

689 **References**

690 Andrew, M., Morton, J.D., Liefering, M. and Bisset, L. (1992) The partitioning of nitrate
691 assimilation between root and shoot of a range of temperate cereals and pasture grasses.
692 *Ann. Bot.* 70: 271-276.

693

694 Aoki, Y., Okamura, Y., Tadaka, S., Kinoshita, K. and Obayashi, T. (2016) ATTED-II in
695 2016: a plant coexpression database towards lineage-specific coexpression. *Plant Cell*
696 *Physiol.* Doi: 10.1093/pcp/pcv165.

697

698 Araya, T., Miyamoto, M., Wibowo, J., Suzuki, A., Kojima, S., Tsuchiya, Y.N., Sawa, S.,
699 Fukuda, H., von Wirén, N. and Takahashi, H. (2014) CLE-CLAVATA1 peptide-receptor
700 signaling module regulates the expansion of plant root systems in a nitrogen-dependent
701 manner. *Proc. Natl. Acad. Sci. USA* 111: 2029-2034.

702

703 Bloom, A.J., Burger, M., Asensio, J.S.R. and Cousins, A.B. (2010) Carbon dioxide
704 enrichment inhibits nitrate assimilation in wheat and *Arabidopsis*. *Science* 328: 899-903.

Bräutigam, A., Gagneul, D. and Weber, A.P.M. (2007) High-throughput colorimetric method for the parallel assay of glyoxylic acid and ammonium in a single extract. *Anal. Biochem.* 362: 151–153.

Clough, S.J. and Bent, A.F. (1998) Floral dip: a simplified method for *Agrobacterium*-mediated transformation of *Arabidopsis thaliana*. *Plant J.* 16: 735-743.

Duan, Z., Homma, A., Kobayashi, M., Nagata, N., Kaneko, Y., Fujiki, Y. and Nishida, I. (2014) Photoassimilation, assimilate translocation and plasmodesmal biogenesis in the source leaves of *Arabidopsis thaliana* grown under an increased atmospheric CO_2 concentration. *Plant Cell Physiol.* 55: 358-369.

Fernández-Marcos, M., Sanz, L. and Lorenzo, O. (2012) An emerging regulator of cell elongation during primary root growth. *Plant Signal. Behav.* 7: 196-200.

Guan, M., Møller, I.S. and Schjoerring, J.K. (2015) Two cytosolic glutamine synthetase isoforms play specific roles for seed germination and seed yield structure in *Arabidopsis*. *J. Exp. Bot.* 66: 203-212.

Hachiya, T., Watanabe, C.K., Fujimoto, M., Ishikawa, T., Takahara, K., Kawai-Yamada, M. et al. (2012) Nitrate addition alleviates ammonium toxicity without lessening

727 ammonium accumulation, organic acid depletion and inorganic cation depletion in
728 Arabidopsis thaliana shoots. *Plant Cell Physiol*. 53: 577–591.
729
730 Hachiya, T., Sugiura, D., Kojima, M., Sato, S., Yanagisawa, S., Sakakibara, H.,
731 Terashima, I. and Noguchi, K. (2014) High CO_2 triggers preferential root growth of
732 Arabidopsis thaliana via two distinct systems under low pH and low N stresses. *Plant*
733 *Cell Physiol*. 55: 269–280.
734
735 Hanke, G.T., Kimata-Ariga, Y., Taniguchi, I. and Hase, T. (2004) A post genomic
736 characterization of Arabidopsis ferredoxins. *Plant Physiol.* 134: 255-264.
737
738 Hanke, G.T., Okutani, S., Satomi, Y., Takao, T., Suzuki, A. and Hase, T. (2005) Multiple
739 iso-proteins of FNR in *Arabidopsis*: evidence for different contributions to chloroplast
740 function and nitrogen assimilation. *Plant Cell Environ.* 28: 1146-1157.
741
742 Hanke, G.T. and Mulo, P. (2013). Plant type ferredoxins and ferredoxin-dependent
743 metabolism. *Plant Cell Environ.* 36: 1071-1084.
744
745 Hong, S.M., Bahn, S.C., Lyu, A., Jung, H.S. and Ahn, J.H. (2010) Identification and
746 testing of superior reference genes for a starting pool of transcript normalization in
747 Arabidopsis. *Plant Cell Physiol.* 51: 1694-1706.
748

749 Huang, X., von Rad, U. and Durner, J. (2002) Nitric oxide induces transcriptional
750 activation of the nitric oxide-tolerant alternative oxidase in *Arabidopsis* suspension cells.
751 *Planta* 215: 914-923.
752
753 Ishiyama, K., Inoue, E., Watanabe-Takahashi, A., Obara, M., Yamaya, T. and Takahashi,
754 H. (2004) Kinetic properties and ammonium-dependent regulation of cytosolic
755 isoenzymes of glutamine synthetase in *Arabidopsis*. *J. Biol. Chem.* 279: 16598-16605.
756
757 Jefferson, R.A. (1987) Assaying chimeric genes in plants: the GUS gene fusion system.
758 *Plant Mol. Biol. Rep.* 5: 387-405.
759
760 Jones, R.D. and Schwab, A.P. (1993) Nitrate leaching and nitrite occurrence in a fine-
761 textured soil. *Soil Sci.* 155: 272-281.
762
763 Kamada-Nobusada, T., Makita, N., Kojima, M. and Sakakibara, H. (2013) Nitrogen-
764 dependent regulation of de novo cytokinin biosynthesis in rice: the role of glutamine
765 metabolism as an additional signal. *Plant Cell Physiol.* 54: 1881–1893.
766
767 Kiba, T., Henriques, R., Sakakibara, H. and Chua, N.H. (2007) Targeted degradation of
768 PSEUDO-RESPONSE REGULATOR5 by a SCFZTL complex regulates clock function
769 and photomorphogenesis in Arabidopsis thaliana. *Plant Cell* 19 : 2516
770

771 Kiba, T. and Krapp, Anne. (2016) Plant nitrogen acquisition under low availability:
772 regulation of uptake and root architecture. *Plant Cell Physiol.* Doi: 10.1093/pcp/pcw052
773
774 Konishi, M. and Yanagisawa, S. (2011) The regulatory region controlling the nitrate-
775 responsive expression of a nitrate reductase gene, *NIA1*, in Arabidopsis. *Plant Cell*
776 *Physiol.* 52: 824-836.
777
778 Konishi, M. and Yanagisawa, S. (2013) Arabidopsis NIN-like transcription factors have
779 a central role in nitrate signaling. *Nat. Commun.* 4: 1617.
780
781 Konishi, N., Ishiyama, K., Matsuoka, K., Maru, I., Hayakawa, T., Yamaya, T. and Kojima,
782 S. (2014) NADH-dependent glutamate synthase plays a crucial role in assimilation
783 ammonium in the Arabidopsis root. *Physiol. Plant* 152: 138-151.
784
785 Kotur, Z., Siddiqi, Y.M. and Glass, A.D.M. (2013) Characterization of nitrite uptake in
786 *Arabidopsis thaliana*: evidence for a nitrite-specific transporter. *New Phytol.* 200: 201-
787 210.
788
789 Krapp, A., Berthomé, R., Orsel, M., Mercey-Boutet, S., Yu, A., Castaings, L., Elftieh, S.,
790 Major, H., Renou, J.-P. and Daniel-Vedele, F. (2011) Arabidopsis roots and shoots show
791 distinct temporal adaptation patterns toward nitrogen starvation. *Plant Physiol.* 157:
792 1255-1282.

Krapp, A. (2015) Plant nitrogen assimilation and its regulation: a complex puzzle with missing pieces. *Curr. Opin. Plant Biol.* 25: 115-122.

Lancien, M., Martin, M., Hsieh, M.-H., Leustek, T., Goodman, H. and Coruzzi, G. (2002) Arabidopsis *glt1*-T mutant defines a role for NADH-GOGAT in the non-photorespiratory ammonium assimilatory pathway. *Plant J.* 29: 347-358.

Li, G., Dong, G., Li, B., Li, Q., Kronzucker, H.J. and Shi, W. (2012) Isolation and characterization of a novel ammonium overly sensitive mutant, amos2, in Arabidopsis thaliana. *Planta* 235: 239-252.

Lindermayr, C., Saalbach, G. and Durner, J. (2005) Proteomic identification of S-nitrosylated proteins in Arabidopsis. *Plant Physiol.* 137: 921-930.

Lima, J.E., Kojima, S., Takahashi, H. and von Wirén, N. (2010) Ammonium triggers lateral root branching in *Arabidopsis* in an AMMONIUM TRANSPORTER1;3-dependent manner. *Plant Cell* 22: 3621-3633.

Lintala, M., Allahverdiyeva, Y., Kangasjärvi, S., Lehtimäki, N., Keränen, M., Rintamäki, E., Aro, E.-M. and Mulo, P. (2009) Comparative analysis of leaf-type ferredoxin-$NADP^+$ oxidoreductase isoforms in *Arabidopsis thaliana*. *Plant J* 57: 1103-1115.

Lintala, M., Lehtimäki, N., Benz, J.P., Jungfer, A., Soll, J., Aro, E.-M., Bölter, B. and Mulo, P. (2012) Depletion of leaf-type ferredoxin-$NADP^+$ oxidoreductase results in the permanent induction of photoprotective mechanisms in Arabidopsis chloroplasts. *Plant J.* 70: 809-817.

López Pasquali, C.E., Fernández Hernando, P. and Durand Alegría, J.S. (2007) Spectrophotometric simultaneous determination of nitrite, nitrate and ammonium in soils by flow injection analysis. *Anal. Chim. Acta* 600: 177-182.

Lothier, J., Gaufichon, L., Sormani, R., LemaÎtre, T., Azzopardi, M., Morin, H., Chardon, F., Reisdorf-Cren, M., Avice, J.-C. and Masclaux-Daubresse, C. (2011) The cytosolic glutamine synthetase GLN1;2 plays a role in the control of plant growth and ammonium homeostasis in *Arabidopsis* rosettes when nitrate supply is not limiting. *J. Exp. Bot.* 62: 1375-1390.

Maeda, S.-I., Konishi, M., Yanagisawa, S. and Omata, T. (2014) Nitrite transport activity of a novel HPP family protein conserved in cyanobacteria and chloroplasts. *Plant Cell Physiol.* 55: 1311-1324.

Miller, A.J., Fan, X., Orsel, M., Smith, S.J. and Wells, D.M. (2007) Nitrate transport and signaling. *J. Exp. Bot.* 58: 2297-2306.

837

838 Murashige, T. and Skoog, F. (1962) A revised medium for rapid growth and bio assays
839 with tobacco tissue cultures. *Physiol. Plant.* 15: 473-497.

840

841 Obayashi, T., Okamura, Y., Ito, S., Tadaka, S., Aoki, Y., Shirota, M. and Kinoshita, K.
842 (2014) ATTED-II in 2014: Evaluation of gene coexpression in agriculturally important
843 plants. *Plant Cell Physiol.* 55: e6(1-7).

844

845 Onda, Y., Matsumura, T., Kimata-Ariga, Y., Sakakibara, H., Sugiyama, T. and Hase, T.
846 (2000) Differential interaction of maize root ferredoxin:$NADP^+$ oxidoreductase with
847 photosynthetic and non- photosynthetic ferredoxin isoproteins. *Plant Physiol.* 123: 1037-
848 1046.

849

850 Patterson, K., Cakmak, T., Cooper, A., Lager, I., Rasmusson, A.G. and Escobar, M.A.
851 (2010) Distinct signaling pathways and transcriptome response signatures differentiate
852 ammonium- and nitrate-supplied plants. *Plant Cell Environ.* 33: 1486-1501.

853

854 Rachmilevitch, S., Cousins, A.B. and Bloom, A.J. (2004) Nitrate assimilation in plant
855 shoots depends on photorespiration. *Proc. Natl. Acad. Sci. USA* 101: 11506-11510.

856

857 Remans, T., Nacry, P., Pervent, M., Filleur, S., Diatloff, E., Mounier, E., Tillard, P., Forde,
858 B.G. and Gojon, A. (2006) The *Arabidopsis* NRT1.1 transporter participates in the

signaling pathway triggering root colonization of nitrate-rich patches. *Proc. Natl. Acad. Sci. USA* 103: 19206-19211.

Riley, W.J., Ortiz-Monasterio, I. and Matson, P.A. (2001) Nitrogen leaching and soil nitrate, nitrite, and ammonium levels under irrigated wheat in Northern Mexico. *Nutr. Cycl. Agroecosys.* 61: 223-236.

Rockel, P., Strube, F., Rockel, A., Wildt, J. and Kaiser, W.M. (2002) Regulation of nitric oxide (NO) production by plant nitrate reductase *in vivo* and *in vitro*. *J. Exp. Bot.* 53: 103-110.

Samater, A.H., Van Cleemput, O. and Ertebo, T. (1998) Influence of the presence of nitrite and nitrate in soil on maize biomass production, nitrogen immobilization and nitrogen recovery. *Biol. Fertil. Soils* 27: 211-218.

Scheurwater, I., Koren, M., Lambers, H. and Atkin, O.K. (2002) The contribution of roots and shoots to whole plant nitrate reduction in fast- and slow-growing grass species. *J. Exp. Bot.* 53: 1635-1642.

Shen, Q.R., Ran, W. and Cao, Z.H. (2003) Mechanisms of nitrite accumulation occurring in soil nitrification. *Chemosphere* 50: 747-753.

881 Taira, M., Valtersson, U., Burkhardt, B. and Ludwig, R.A. (2004) *Arabidopsis thaliana*
882 *GLN2*-encoded glutamine synthetase is dual targeted to leaf mitochondria and
883 chloroplasts. *Plant Cell* 16 :2048-2058.
884
885 Wang, R., Guegler, K., LaBrie, S.T. and Crawford, N.M. (2000) Genomic analysis of a
886 nutrient response in Arabidopsis reveals diverse expression patterns and novel metabolic
887 and potential regulatory genes induced by nitrate. *Plant Cell* 12: 1491-1509.
888
889 Wang, R., Okamoto, M., Xing, X. and Crawford, N.M. (2003) Microarray analysis of the
890 nitrate response in Arabidopsis roots and shoots reveals over 1,000 rapidly responding
891 genes and new linkages to glucose, trehalose-6-phosphate, iron, and sulfate metabolism.
892 *Plant Physiol.* 132: 556-567.
893
894 Wang, R., Xing, X. and Crawford, N. (2007) Nitrite acts as a transcriptome signal at
895 micromolar concentrations in Arabidopsis roots. *Plant Physiol.* 145: 1735-1745.
896
897 Wang, R., Xing, X., Wang, Y., Tran, A. and Crawford, N.M. (2009) A genetic screen for
898 nitrate regulatory mutants captures the nitrate transporter gene NRT1.1. *Plant Physiol.*
899 151: 472-478.
900
901 Wilkinson, J.Q. and Crawford, N.M. (1993) Identification and characterization of a
902 chlorate-resistant mutant of *Arabidopsis thaliana* with mutations in both nitrate reductase

structural genes *NIA1* and *NIA2*. *Mol. Gen. Genet.* 239: 289-297.

Yu, X., Sukumaran, S. and Márton, L. (1998) Differential expression of the Arabidopsis *Nia1* and *Nia2* genes. *Plant Physiol.* 116: 1091-1096.

925

926

927

928 **Legends to figures**

929 **Fig. 1** RFNR2 is the major RFNR isoform in roots grown on nitrite media. (A) Schematic
930 representation of *rfnr1* and *rfnr2* T-DNA insertion alleles. Boxes represent exons;
931 horizontal thin bars, untranslated region; horizontal thick bars, introns; ATG, initiation
932 codon; TGA, termination codon. (B) RT-PCR analysis using specific primers of *RFNR1*
933 and *RFNR2* transcript levels in roots of Col, *rfnr1* and *rfnr2-2* mutants grown under 0.2
934 mM nitrite for seven days (Supplementary Table S2). *ACT2* was used as the loading
935 control. (C) Immunodetection of RFNR1 and RFNR2 isoproteins with specific antisera
936 raised against maize RFNR following SDS-PAGE and western blotting in roots of Col,
937 *rfnr1* and *rfnr2-2* mutants grown under 0.2 mM nitrite for seven days. The position of the
938 nearest molecular weight marker is given on the left.

939

940 **Fig. 2** *RFNR2* is induced by nitrite. (A) Absolute transcript levels of *RFNR1* and *RFNR2*
941 in shoots and roots of Col grown under 0.2mM of nitrate (NA), nitrite (NI) or ammonium
942 (A) for seven days (Mean ± SD, n = 3). (B) Relative transcript levels of *RFNR2* in 7 d
943 Col roots before (0 min) or after (30 min) the transfer to 0.2 mM nitrate, nitrite or
944 ammonium (Mean ± SD, n = 3). (C) The tissue specific pattern of GUS activity in 5-day-
945 old *pRFNR2::GUS* seedlings grown under nitrate or nitrite. The arrowheads indicate root
946 tips. The scale bar denotes 10 mm. (D) GUS activity in the central portion of the primary

947 root. The scale bar denotes 100 μm. (E) GUS activity in the primary root tips. The scale
948 bar denotes 50 μm. (F) Relative transcript levels of *RFNR2* and *GUS* in the roots of 5 d
949 *pRFNR2::GUS* seedlings grown under nitrate or nitrite (Mean ± SD, n = 4). Tukey-
950 Kramer's multiple comparison test was conducted at a significance level of $P < 0.05$ only
951 when a one-way ANOVA was significant at $P < 0.05$. Different letters denote significant
952 differences. Student's *t*-test was conducted (*$P < 0.05$).
953
954 **Fig. 3** *RFNR2* is essential for normal root growth on nitrite media. (A) Representative
955 photographs in 9-day-old Col and *rfnr2-2* grown on media containing 0.2 mM nitrate,
956 nitrite or ammonium. (B) Primary root length in 7-day-old Col and *rfnr2-2* grown on 0.2
957 mM nitrate (NA), nitrite (NI) or ammonium (A) (Mean ± SD, n = 10). White and black
958 bars denote Col and *rfnr2-2*, respectively. (C) Lateral root length in 7-day-old Col and
959 *rfnr2-2* grown on 0.2 mM nitrate, nitrite or ammonium (Mean ± SD, n = 10). (D)
960 Concentration dependency of primary root length in 7-day-old Col and *rfnr2-2* grown on
961 0, 0.04, 0.2 and 1 mM nitrate or nitrite (Mean ± SD, n = 12-15). (E) Time-courses of
962 primary root elongation per day on 0.2 mM of each N source (Mean ± SD, n = 15). (F)
963 Primary root elongation 3 days after the transfer from 0.2 mM nitrate or nitrite to 0.2 mM
964 of nitrate or nitrite in 4-day-old Col and *rfnr2-2*. "NA to NA" means the transfer from 0.2
965 mM nitrate to 0.2 mM nitrate (Mean ± SD, n = 5). Tukey-Kramer's multiple comparison
966 test was conducted at a significance level of $P < 0.05$ only when a one-way ANOVA was
967 significant at $P < 0.05$. Different letters denote significant differences. NS means not
968 significant.

969

970 **Fig. 4** Impaired root growth of *RFNR2* mutant is due to nitrite accumulation. (A) Nitrite
971 contents in roots of 7-day-old Col and *rfnr2-2* grown on 0.2 mM nitrate (NA) or nitrite
972 (NI) (Mean ± SD, n = 3). White and black bars denote Col and *rfnr2-2*, respectively. (B)
973 Primary root length in 7-day-old Col and *rfnr2-2* grown on 0.2 mM nitrite in the presence
974 or absence of the NO scavenger, cPTIO (Mean ± SD, n = 10). (C) Relative transcript
975 levels of *AOX1a* in roots of 7-day-old Col and *rfnr2-2* grown on 0.2 mM nitrate or nitrite
976 (Mean ± SD, n = 3). (D) NR activities (NRA) in shoots and roots of 7-day-old Col grown
977 on 0.2 mM nitrite (Mean ± SD, n = 3). (E) Protein contents in plants of 7-day-old Col and
978 *rfnr2-2* grown on 0.2 mM nitrate, nitrite or ammonium (Mean ± SD, n = 3). (F) Primary
979 root length in 7-day-old Col and *rfnr2-2* under 0.2 mM of nitrate, 0.2 mM nitrate plus 0.2
980 mM nitrite (i.e. 0.4 mM N in total), 0.2 mM nitrite, 0.2 mM nitrite plus 0.2 mM of
981 ammonium (i.e. 0.4 mM N in total) or 0.2 mM ammonium (Mean ± SD, n = 10). (G)
982 Representative photographs in 7-day-old Col and *rfnr2-2* grown on 0.2 mM nitrate, 0.2
983 mM nitrate plus 0.2 mM nitrite or 0.2 mM nitrite. Tukey-Kramer's multiple comparison
984 test was conducted at a significance level of $P < 0.05$ only when a one-way ANOVA was
985 significant at $P < 0.05$. Different letters denote significant differences. ND and NS mean
986 not detected and not significant, respectively.

987

988 **Fig. 5** A specific set of genes related to nitrite reduction uniformly responds to nitrite. (A)
989 Relative transcript levels of *NIR*, *FD3*, *G6PD2*, *G6PD3*, *At1g64190*, *At5g41670* and
990 *At4g34270* (a reference gene, Hong et al. 2010) in shoots and roots of 7-day-old Col

991 grown on 0.2mM nitrate (NA), nitrite (NI) or ammonium (A) for seven days (Mean ± SD,
992 n = 3). (B) Relative transcript levels of *NIR*, *FD3*, *G6PD2*, *G6PD3*, *At1g64190*,
993 *At5g41670*, *RFNR1* and *At4g34270* in 7-day-old Col roots before (0 min) or after (30
994 min) transfer to 0.2 mM nitrate, nitrite or ammonium (Mean ± SD, n = 3). (C) Relative
995 transcript levels of *NIR*, *FD3*, *G6PD2*, *G6PD3*, *At1g64190*, *At5g41670*, *RFNR1* and
996 *At4g34270* in roots of 7-day-old Col and *rfnr2-2* grown on 0.2mM nitrite (Mean ± SD, n
997 = 3). White and black bars denote Col and *rfnr2-2*, respectively. Tukey-Kramer's multiple
998 comparison test was conducted at a significance level of $P < 0.05$ only when a one-way
999 ANOVA was significant at $P < 0.05$. Student's *t*-test was conducted (*$P < 0.05$). NS
1000 means not significant.
1001
1002 **Fig. 6** RFNR2 is not essential for N reduction/assimilation when nitrate or ammonium
1003 are the sole N sources. (A) NR activities (NRA) in shoots and roots of 7-day-old Col on
1004 0.2 mM nitrate (Mean ± SD, n = 4). (B) Nitrate contents in shoots and roots of 7-day-old
1005 Col and NR double mutant (*nr*) on 0.2 mM nitrate (Mean ± SD, n = 3). White and dotted
1006 bars denote Col and *nr*, respectively. (C) GS activities in roots of 7-day-old Col and *gln1;2*
1007 grown on 0.2mM ammonium (Mean ± SD, n = 4). White and diagonal bars denote Col
1008 and *gln1;2*, respectively. (D) Ammonium contents in the roots of 7-day-old Col and
1009 *gln1;2* grown on 0.2 mM ammonium (Mean ± SD, n = 3). (E) Contents of glutamine and
1010 glutamate in roots of 7-day-old Col and *rfnr2-2* grown on 0.2 mM ammonium (Mean ±
1011 SD, n = 3). White and black bars denote Col and *rfnr2-2*, respectively. Tukey-Kramer's
1012 multiple comparison test was conducted at a significance level of $P < 0.05$ only when a

1013 one-way ANOVA was significant at $P < 0.05$. Different letters denote significant
1014 differences. Student's *t*-test was conducted ($*P < 0.05$). ND and NS mean not detected
1015 and not significant, respectively.

Figure 1

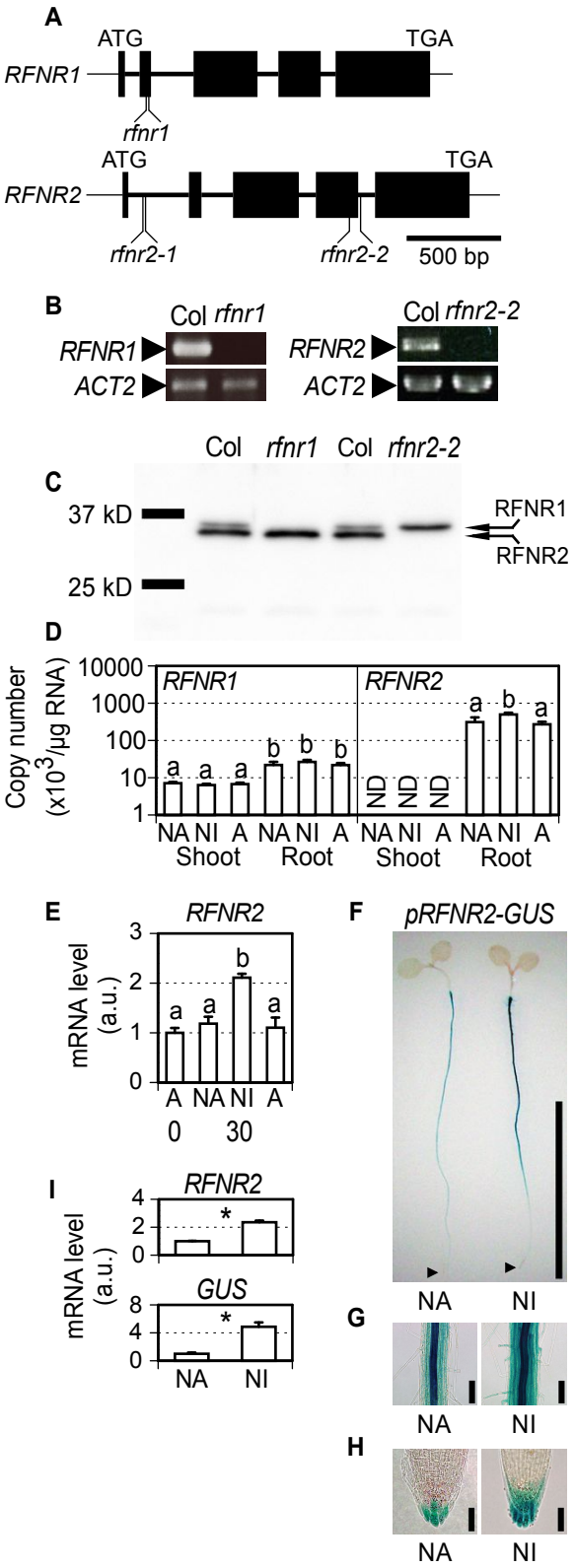
A
ATG
TGA
RFNR1
rfnr1
ATG
TGA
RFNR2
rfnr2-1
rfnr2-2
500 bp
B
Col rfnr1
Col rfnr2-2
RFNR1
ACT2
RFNR2
ACT2
Col rfnr1 Col rfnr2-2
C
37 kD
25 kD
RFNR1
RFNR2
D
Copy number (x10^3/µg RNA)
RFNR1
RFNR2
NA NI A NA NI A NA NI A NA NI A
Shoot Root Shoot Root
E
RFNR2
mRNA level (a.u.)
A NA NI A
0 30
F
pRFNR2-GUS
NA NI
G
NA NI
H
NA NI
I
RFNR2
GUS
mRNA level (a.u.)
NA NI

Figure 2

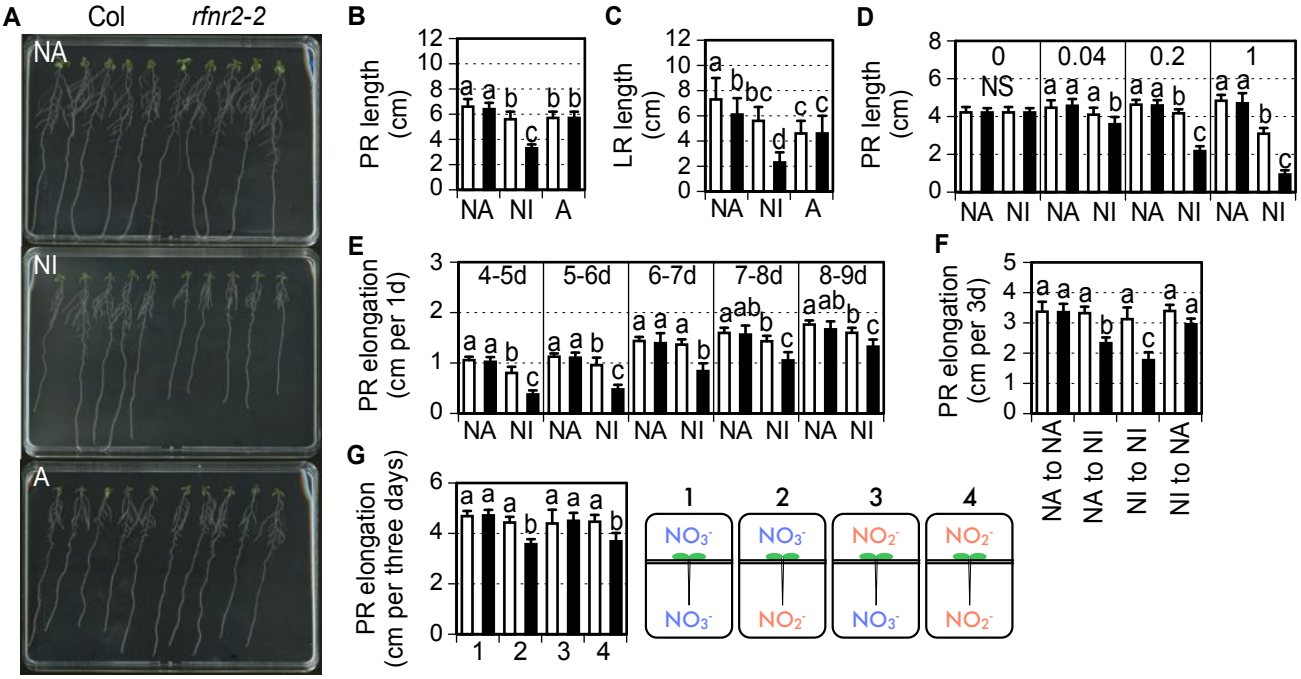
A
Col
rfnr2-2
NA
NI
A
B
PR length (cm)
NA NI A
C
LR length (cm)
NA NI A
D
PR length (cm)
0
NS
0.04
0.2
1
NA NI NA NI NA NI NA NI
E
PR elongation (cm per 1d)
4-5d
5-6d
6-7d
7-8d
8-9d
NA NI NA NI NA NI NA NI NA NI
F
PR elongation (cm per 3d)
NA to NA
NA to NI
NI to NI
NI to NA
G
PR elongation (cm per three days)
1 2 3 4
1
2
3
4
NO3-
NO2-

Figure 3

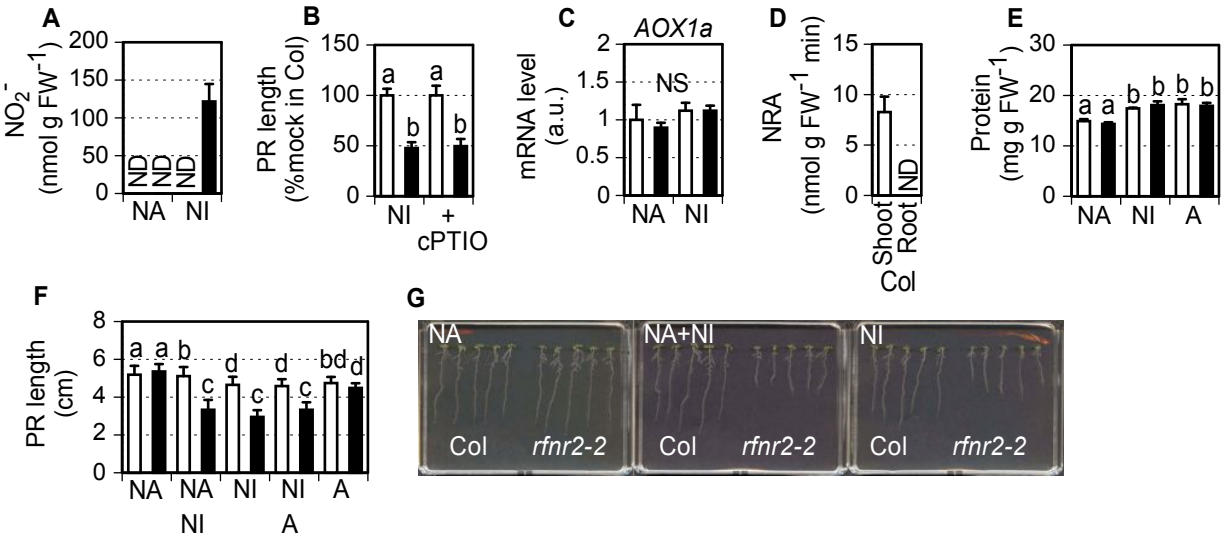
A
NO_2^- (nmol g FW^{-1})
200
150
100
50
0
ND
ND
ND
NA
NI
B
PR length (%mock in Col)
150
100
50
0
a
b
a
b
NI
+ cPTIO
C
AOX1a
mRNA level (a.u.)
2
1.5
1
0.5
0
NS
NA
NI
D
NRA (nmol g FW^{-1} min)
15
10
5
0
Shoot
Root
ND
Col
E
Protein (mg g FW^{-1})
30
20
10
0
a
a
b
b
b
b
NA
NI
A
F
PR length (cm)
8
6
4
2
0
a
a
b
c
d
c
d
c
bd
d
NA
NA
NI
NI
A
NI
A
G
NA
NA+NI
NI
Col
rfnr2-2
Col
rfnr2-2
Col
rfnr2-2

Figure 4

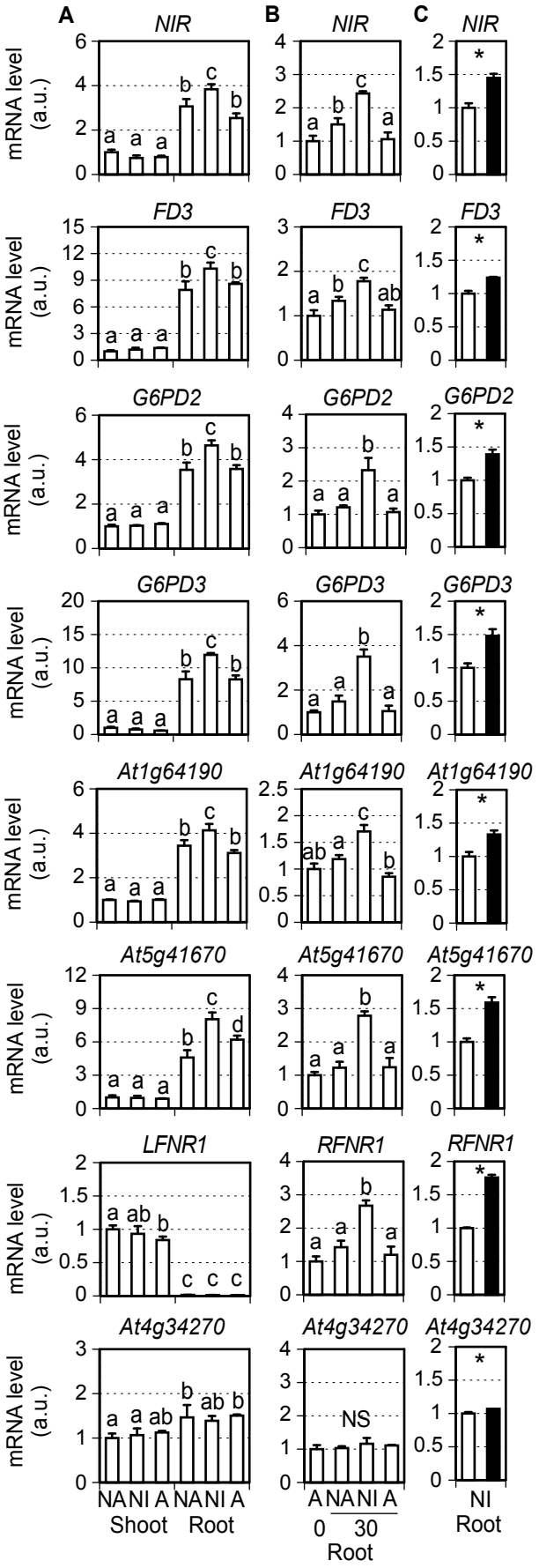
A
B
C
NIR
FD3
G6PD2
G6PD3
At1g64190
At5g41670
LFNR1
RFNR1
At4g34270
mRNA level (a.u.)
NS
N A NI A N A NI A
Shoot Root
A N A NI A
0 30
Root
NI
Root

Figure 5

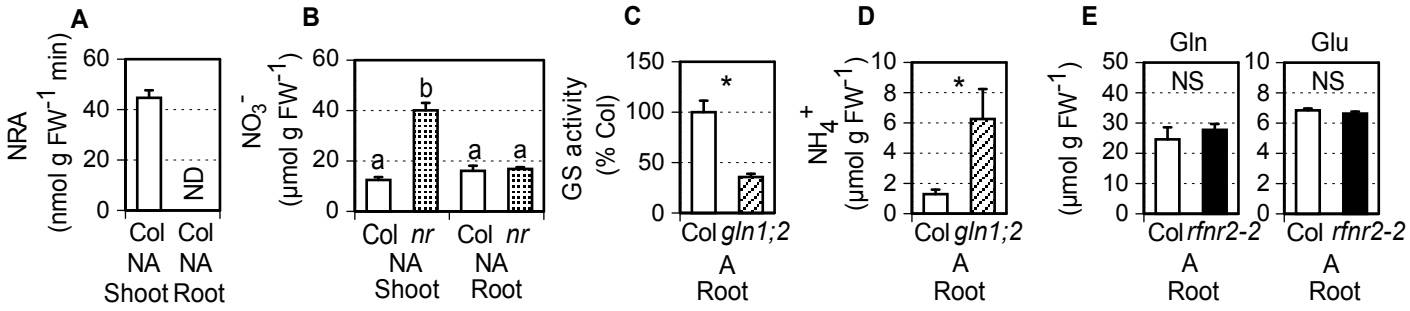
A
NRA (nmol g FW-1 min)
60
40
20
0
ND
Col
NA
Shoot
Col
NA
Root
B
NO3-
(µmol g FW-1)
60
40
20
0
a
b
a
a
Col
nr
NA
Shoot
Col
nr
NA
Root
C
GS activity (% Col)
150
100
50
0
*
Col
gln1;2
A
Root
D
NH4+
(µmol g FW-1)
10
8
6
4
2
0
*
Col
gln1;2
A
Root
E
Gln
Glu
(µmol g FW-1)
50
40
30
20
10
0
10
8
6
4
2
0
NS
NS
Col
rfnr2-2
A
Root
Col
rfnr2-2
A
Root

Table S1. A list coexpressed with RFNR2 by ATTED II (Obayashi et al. 2007)

AGI No.	AGI No.	Gene name
1st	At1g24280	*G6PD3*
2nd	At5g41670	*dehydrogenase*
3rd	At5g13420	*TRA2*
4th	At4g05390	*RFNR1*
5th	At1g78050	*PGM*
6th	At5g13110	*G6PD2*
7th	At2g15620	*NIR*
8th	At1g63940	*MDAR6*
9th	At2g27510	*FD3*
10th	At1g64190	*dehydrogenase*

Table S2. Primer seqences

AGI No.	Gene name	Purpose	Primer 1 (5'->3')	Primer 2 (5'->3')	Reference
AT4G05390	*RFNR1*	gPCR for SALK_085009	TAACAACGAATTTGGCTTTGG	GGGATTCTCACCCTACGAGTC	This paper
AT1G30510	*RFNR2*	gPCR for SAIL_527_G10	CCAACTACTCGCTCCACAGAG	TCGGTTCAGGAAAATGATTTG	This paper
AT1G30510	*RFNR2*	gPCR for SALK_133654	TCAATAGACTTCAACGTGCCAC	CTCTGTGGAGCGAGTAGTTGG	This paper
AT3G18780	*ACT2*	RT-PCR/gPCR	TGTCCTCCTCACTTTCATCAGC	CATCAATTCGATCACTCAGAGC	This paper
AT4G05390	*RFNR1*	RT-PCR/gPCR	CACCATGGCTCTCTCAACTACTCCTTC	TCAATACACTTCAACATGCCACTGC	This paper
AT1G30510	*RFNR2*	RT-PCR/gPCR	CACCATGTCTCACTCTGCTGTTTC	TCAATAGACTTCAACGTGCCACTG	This paper
AT3G53750	*ACT3*	Q-PCR	GGCTAACCGTGAGAAGATGA	CGACCTGCAAGATCAAGACG	Watanabe et al. (2014)
AT3G22370	*AOX1a*	Q-PCR	CCGATTTGTTCTTCCAGAGG	GCGCTCTCTCGTACCATTTC	Escobar et al. (2004)
AT1G64190	*At1g64190*	Q-PCR	GCACTATCCCGAATCGGTCTC	AGGCGAGGTTTTGGCCCAT	This paper
AT4G34270	*At4g34270*	Q-PCR	CATTTCAGTCTCTATCTGCGAAAGGGTATCC	CACCACAATAAGTCAGTGGAGTAACTCCTTAC	Hong et al. (2010)
AT5G41670	*At5g41670*	Q-PCR	GAGTCAGTAAAGCATGGACACAGT	AGCTGAAACAATTTGTTTTCGTGTTCT	Gonzali et al. (2006)
AT2G27510	*FD3*	Q-PCR	GCAGCTGAAGAGGCAGGAGT	AAGTAGAACACGCACCGGCT	This paper
AT5G13110	*G6PD2*	Q-PCR	CCCTGGTTTAGGAATGAGAT	TAAGAGAAACCCCTTTGGTT	Wakao and Benning (2005)
AT1G24280	*G6PD3*	Q-PCR	TGGTTTATGGAAACTTTCTTTCGC	AGGGTGGCAAGAATAGGGTA	Ruffel et al. (2011)
AT1G66200	*GLN1;2*	Q-PCR	AGCCAAGCTTCTCGATCGCC	TGGAATGGAGCTGGTGCTCA	This paper
AT5G35630	*GLN2*	Q-PCR	TTGACCAGTTCTCATGGGGC	TTAGATGCTGGACGGCGATC	This paper
AT5G53460	*GLT*	Q-PCR	TTGGACCTGAGCCAACACTTG	CATCATCCGTTTTGGTGAGGA	Potel et al. (2009)
AT5G04140	*GLU1*	Q-PCR	ATCATTCAAGAGCAGGTTGT	GACAGTTGAAAGCAGTTATT	Potel et al. (2009)
AT2G41220	*GLU2*	Q-PCR	TACACATTTGATCGTGGTTT	AATCGAAAACCCTTTCTTAA	Potel et al. (2009)
-	*GUS*	Q-PCR	GAAAGCGCGTTACAAGAAAG	GACGTTGCCCGCATAATTAC	Tanabe et al. (2015)
AT5G66190	*LFNR1*	Q-PCR	CTGCAGTCTCTTTACCTTCTCC	GACAACAATCCCTTCTTCCTGTTTC	Lintala et al. (2009)
AT2G15620	*NIR*	Q-PCR	CATGGGATGCTTAACACGAG	AATGGAACCAACTCCGTGAC	Konishi and Yanagisawa (2011)
AT4G05390	*RFNR1*	Q-PCR	CAATGCCAAACCCGGCGATA	CCTTTCCAGATGGACCGGTGA	This paper
AT1G30510	*RFNR2*	Q-PCR	CGGGCTTTGAATCACATAGG	TGTGATTCCTCCAGGTGAGA	This paper

Figure S1

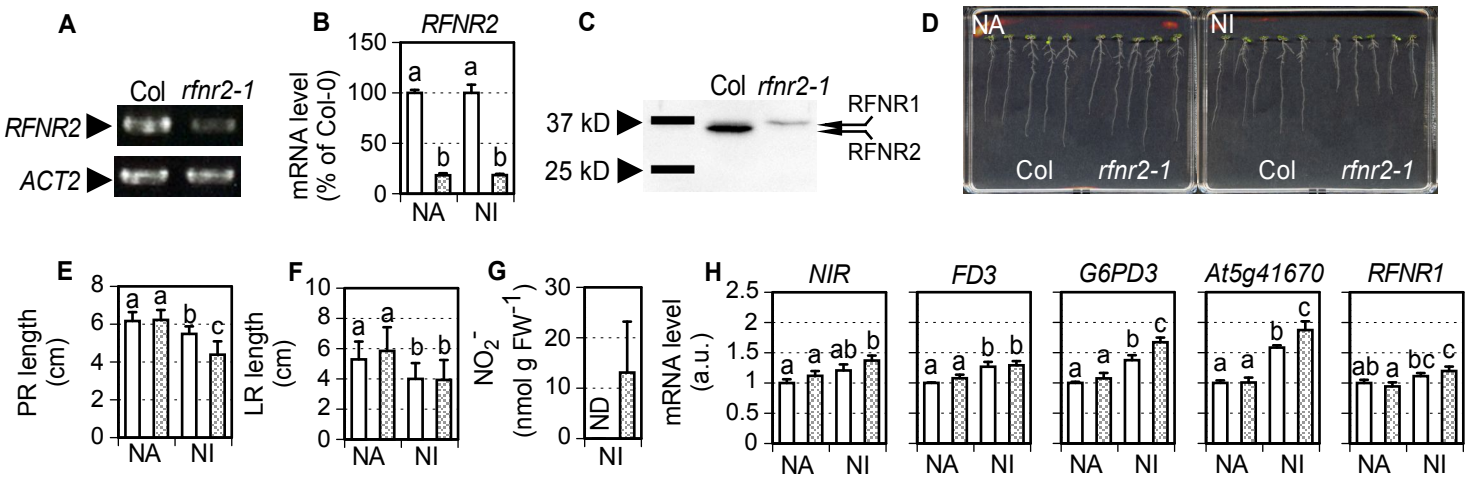
A
Col
rfnr2-1
RFNR2
ACT2
B
RFNR2
mRNA level (% of Col-0)
150
100
50
0
a
a
b
b
NA
NI
C
Col
rfnr2-1
37 kD
25 kD
RFNR1
RFNR2
D
NA
NI
Col
rfnr2-1
Col
rfnr2-1
E
PR length (cm)
LR length (cm)
8
6
4
2
0
a
a
b
c
NA
NI
F
10
8
6
4
2
0
a
a
b
b
NA
NI
G
NO_2^- (nmol g FW^{-1})
30
20
10
0
ND
NI
H
mRNA level (a.u.)
NIR
FD3
G6PD3
At5g41670
RFNR1
2.5
2
1.5
1
0.5
0
a a ab b
a a b b
a a b c
a a b c
ab a bc c
NA
NI

Figure S2

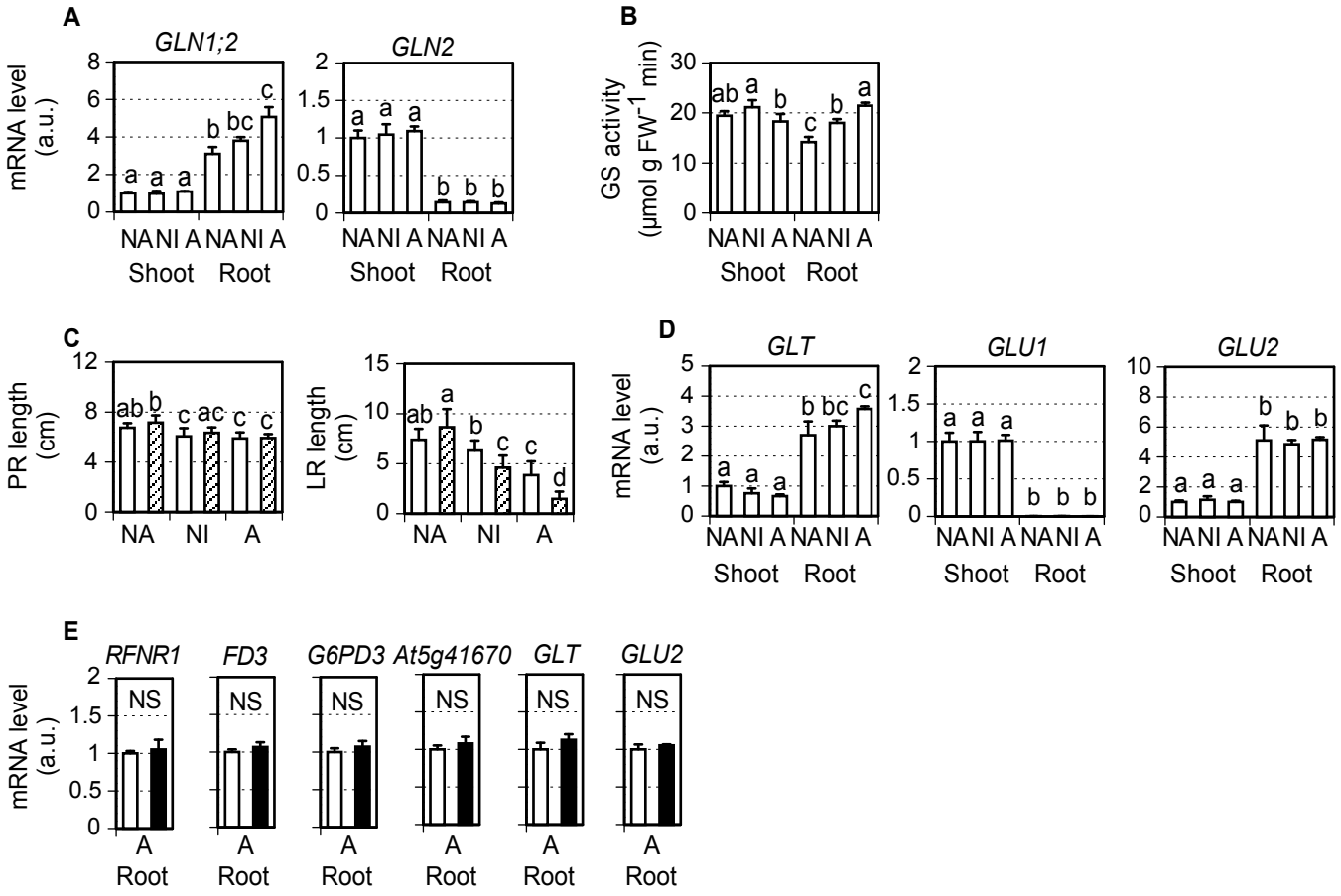
A
GLN1;2
GLN2
mRNA level (a.u.)
NA NI A NA NI A
Shoot Root
B
GS activity (µmol g FW-1 min)
C
PR length (cm)
LR length (cm)
NA NI A
D
GLT
GLU1
GLU2
E
RFNR1
FD3
G6PD3
At5g41670
NS
Root

Figure S3

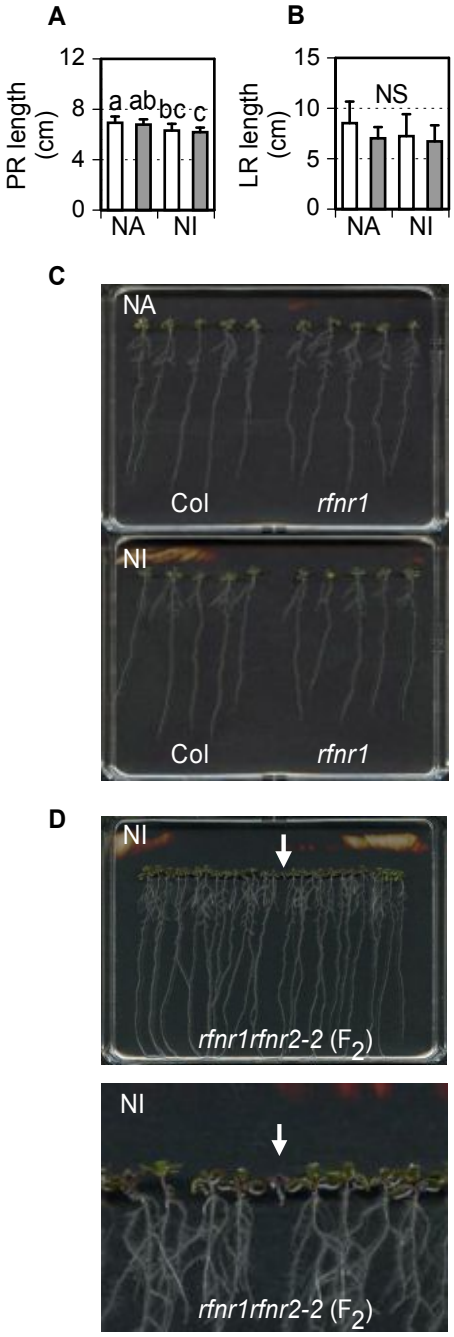
A
B
12
8
4
0
PR length (cm)
a
ab
bc
c
NA
NI
15
10
5
0
LR length (cm)
NS
NA
NI
C
NA
Col
rfnr1
NI
Col
rfnr1
D
NI
rfnr1rfnr2-2 (F2)
NI
rfnr1rfnr2-2 (F2)